ELECTROMAGNETIC CHARACTERISTICS ANALYSIS OF MAGNETIC OBSTACLE LAYER COUPLED PRIMARY PERMANENT MAGNET LINEAR MOTOR FOR RAIL TRANSIT

Xiuping WANG[1*], Shunyu YAO[1], Chunyu QU[1], Xiong YANG[2]

Low power factor and low efficiency are issues with using linear induction motors in rail transportation systems. This paper puts forward a kind of special structure of primary permanent magnet linear motor (PPMLM). Firstly, it introduces the structure and operating mechanism of the motor in detail. Secondly, the air gap flux density equation and the synchronous speed equation are deduced by using the equivalent magnetic circuit method. Thirdly, a 12/8 pole primary permanent magnet linear motor is designed. Parametric modeling and magnetic field analysis are carried out with finite element analysis software, the effect of secondary pole pitch factor and the number of permeance layers on magnetic field modulation capability is obtained, the influence of the thickness of the permanent magnet and the width of the primary opening groove width are analyzed. Finally, it analyzes the magnetic field distribution of PPMLM, then obtains the Fourier decomposition diagram of the back-EMF waveform and air-gap flux density, and the Electromagnetic thrust is studied in detail. It provides a valuable reference for the study of the linear drive motor of rail transit.

Keywords: PPMLM, rail transit, pole pitch factor, finite element method

1. Introduction

The two main driving motors suitable for transportation systems include rotary motor and linear motor. Compared with the drive mode of the rotating motor, simple structure, long life, strong climbing ability are the advantages of the linear motor, small wheel diameter, small cross-section of the tunnel and high degree of freedom of the line design are also its advantages[1-2]. Linear permanent magnet synchronous motor (LPMSM) is more common in the application of the drive motor to the rail transit system. Meanwhile, linear induction motor is also a very prevalent motor used in rail transport system, but this kind of motor has the problems such as poor efficiency and low power factor [3]. Some features like high efficiency, high power density, small volume, good performance are the advantages of LPMSM. For traditional LPMSM, the primary or secondary structure includes armature winding and permanent magnet, and they are placed

*Corresponding author e-mail: wangxpmail@163.com
1 Shenyang Institute of Engineering, Shenyang 110136, China
2 Midea welling Motor Co., Ltd, China

on the different side. So, manufacturing and maintenance costs are high, the application of in City Rail long-distance transportation in applications are limited[4].

Flux switching permanent magnet motor proposed by [5-6] is a new type of motor, although this kind of motor has some good features such as high induction electromotive force and so on, the detent force of this kind of motor is larger, causing greater fluctuation of motor thrust. Professor T.A.Lipo and others put forward a double salient permanent magnet motor based on the switched reluctance motor. This kind of motor is a unipolar permanent magnet flux linkage motor, so its power density is slightly lower than flux-switching permanent magnet motor[7-8]. A permanent magnet vernier motor was a new type of motor which was developed in recent years [9-13], the permanent magnets are attached to the bottom of the primary tooth. Usually, there are several pairs of permanent magnets on each tooth so that the permanent magnets are easy to produce leakage flux between the poles. Vector control is still the main control mode of linear motor, but the application research of direct thrust control technology with simple control structure and good stability is the future research direction[14-16].

The structure optimization of PPMLM can be divided into primary optimization and secondary optimization. Researchers generally believe that permanent magnets placed on the air gap surface has less leakage flux and better performance. The secondary structure plays the role of magnetic field modulation, and its performance directly determines the motor performance. Therefore, the secondary optimization is the key to the optimal design of this type of motor.

A new type of PPMLM is presented in the article (Primary permanent magnet linear machine), referred to as PPMLM. This motor has some advantages such as simple structure, high power factor, and efficient feature comparing to the traditional linear induction motor. Meanwhile, permanent magnets and winding are set on the primary (rotor side), and the track of secondary (stator side) is just made of ordinary magnetic materials. It can significantly reduce manufacturing cost, and almost does not need maintenance, thus this kind of motor presents a great direction of development in rail transportation.

2 The structure of PPMLM

A. Primary

This article introduces the PPMLM, as presented in Fig. 1. The primary core of PPMLM is combination of an ordinary silicon steel sheet, and the convex pole structure is adopted in the secondary. The primary core adopts semi open groove, in which the three-phase armature winding is placed. The armature winding has a logarithmic number of q, and the pole number of the permanent magnet is p_{PM}, in which the poles of the two magnetic fields are not the same. When running, the armature magnetic field and permanent magnet magnetic field

are coupled by secondary magnetic reluctance, realizing the conversion of electromechanical energy. For the primary core of PPMLM, the salient feature structure is permanent magnets and armature windings is that permanent magnets and armature windings are inlaid with each other, thus reducing the cost and improving operational reliability.

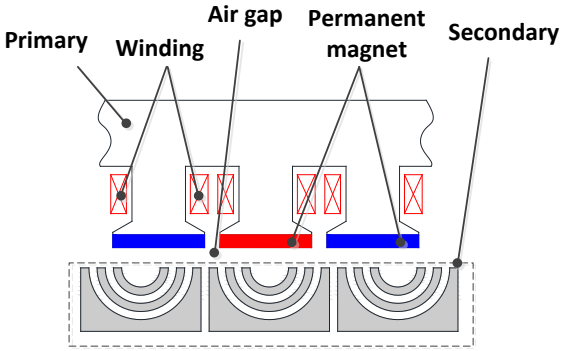

Fig. 1. Sectional diagram of PPMLM

B. Secondary

A radial salient magnetic obstacle structure is used in the secondary structure of PPMLM. N_r is the number of secondary salient poles. It satisfies a relation between the number of permanent magnets and windings, as shown below.

$$N_r = p_{PM} + q \tag{1}$$

In the formula, pPM and q represent the pole-pairs number of the permanent magnets and the armature windings respectively. Fig. 2 presents the secondary structure of PPMLM. The secondary structure also has a magnetic obstacle layer, and the magnetic obstacle layer enables the flux to flow along the path that facilitates electromechanical energy conversion. Considering the function of PPMLM can be influenced by motor structural parameters, we can define a parameter firstly. The definition of pole pitch factor is the length ratio of salient part and each part, and the expression of the pole pitch factor isλ1 /λ2. In this paper, the secondary has neither windings nor permanent magnets, so the structure is simple and reliable, and it is especially suitable for long-distance rail transit system.

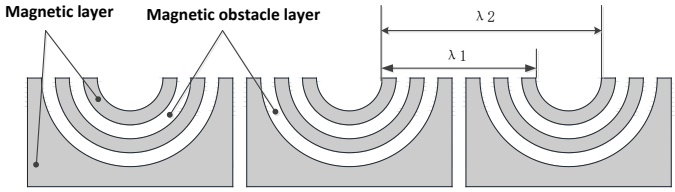

Fig. 2. Secondary structure diagram

3. The working principle of PPMLM

When the motor is in a steady-state, the armature winding creates a moving wave magnetic field along the straight line in the air gap. A permanent magnet produces a relatively stationary magnetic field. The secondary structure of PPMLM modulates two magnetic fields to achieve indirect coupling and creates electromagnetic torque on the primary.

A. Air-gap flux density analysis

Some essential assumptions must be made to simplify the derivation process:

(1) Ignoring core saturation and magnetic leakage.

(2) It is assumed that the relative permeability of permanent magnets is 1.

(3) Assuming that the secondary has the high magnetic permeability, the permeability per unit area is the same, while the flux leakage between the teeth is zero.

When the primary and secondary of PPMLM are relatively stationary, the ideal air gap ratio permeance function can be approximately represented as

$$\lambda_a = \lambda_0 + \sum_{m=1}^{\infty} \lambda_m (\frac{k}{m}) \sin(m\alpha_s \pi) \cos[m \frac{2\pi}{l_t + l_s}(x - x_0)] \tag{2}$$

In the formula, the mean value of air gap magnetic permeability isλ0, and λm means the harmonic amplitude of m order, lt and ls are the secondary teeth and groove length of PPMLM respectively,αs means the pole pitch factor of secondary, k means the modulus of fundamental superimposed magnetic barrier， and x0 is the initial position.

Without considering the higher-order harmonic waves of permeance, the no-load air gap ratio of PPMLM is approximately shown as

$$\lambda_a = \lambda_0 + \lambda_1 k \sin(\alpha_s \pi) \cos[\frac{2\pi}{l_t + l_s}(x - x_0)] \tag{3}$$

When the motor is operated, the coordinates of the air-gap permeance are expressed as

$$\lambda_a(x, t) = \lambda_0 + \lambda_1 k \sin(\alpha_s \pi) \cos[\frac{2\pi}{l_t + l_s}(x - x_0 - v_t t)] \tag{4}$$

Where, vt is the motor’s speed.

In addition, the magneto-motive potential generated by a permanent magnet in an air gap can also be expressed in terms of the Fourier series

$$f_{PM}(x)=\sum_{j=2n-1,n=1}^{\infty}\frac{4B_v h_{PM}}{j\mu_0\pi}\cos\left(jp_{PM}\frac{2\pi}{l_a}x\right) \tag{5}$$

In the formula, for permanent magnet, Bv is Vertical component, hPM means its thickness, pPM means number of pole pairs, meanwhile, La means the primary length, and μ0 is the magnetic permeability in vacuum.

The effect of higher harmonics is ignored, air gap, the permanent magnet creates the magnetomotive force, it can be approximately shown as

$$f_{PM}(x)=\frac{4B_v h_{PM}}{\mu_0\pi}\cos\left(p_{PM}\frac{2\pi}{l_a}x\right) \tag{6}$$

In order to simplify writing, l replaces lt+ls, s replaces sin(αsπ), when the motor is unloaded, the flux density is approximately shown as

$$\begin{aligned}B_a(x,t)&=f_{PM}(x)g\lambda_a(x,t)\\&=\frac{4B_v h_{PM}\lambda_0}{\mu_0\pi}\cos\left(p_{PM}\frac{2\pi}{l_a}x\right)+\\&\frac{2B_v h_{PM}\lambda_1}{\mu_0\pi}ks\cos\left[\left(p_{PM}+\frac{l_a}{l}\right)\frac{2\pi}{L_a}\left(x-\frac{l_a v_t t+l_a x_0}{p_{PM}l+l_a}\right)\right]+\\&\frac{2B_v h_{PM}\lambda_1}{\mu_0\pi}ks\cos\left[\left(p_{PM}-\frac{l_a}{l}\right)\frac{2\pi}{l_a}\left(x+\frac{l_a v_t t+l_a x_0}{p_{PM}l-l_a}\right)\right]\end{aligned} \tag{7}$$

The air gap flux density component is generated directly by the permanent magnet in the first item. Since the armature winding and the permanent magnet are in a relatively static state of motion, the component cannot generate EMF in the winding. In the second and third terms, a convex magnetic barrier modulates the air-gap flux density components. The second terms are short in wavelength and slow in operation. Contrary, the third terms are long in wavelength and fast in operation. According to the principle of counter electromotive force, the amplitude of counter EMF is directly proportional to the change rate of effective air gap flux. Therefore, choosing the air gap magnetic flux density component as the effective harmonic component of PPMLM can make the amplitude of the electrodynamic force increased and the thrust density of the PPMLM improved.

By formula (7), the expressions of pflux and vflux are as follows

$$p_{flux}=\left|P_{PM}-N_r\right| \tag{8}$$

$$v_{flux}=\left|\frac{N_r}{p_{PM}-N_r}\right|\cdot v_t \tag{9}$$

Where Nr=la/l means the pole number of secondary convex, pflux means

the pole logarithm of effective harmonic, vflux is the forward speed of the harmonic. By formula (8), it can be seen that the number of pole pairs of a permanent magnet is very different from the number of pole pairs of the effective harmonic. it can be seen that there is a vast difference between the pole number of a permanent magnet and the effective harmonic. The reason is that the effective harmonic flux component is modulated by secondary convex pole magnetic reluctance. So, the pole number of the armature winding equals the pole number of the useful harmonics. In the 12/8-pole motor, the polar-logarithm of the permanent magnet is 6, the polar-logarithm of the armature winding is 4, and the 10 is the number of secondary convex.

B. The analysis of speed

The linear motor is developed by a rotating motor, and the traveling wave speed in PPMLM is called the synchronous speed of the linear motor.

In a rotating field modulated motor, the synchronous speed of motor [14] is nr

$$n_r = \frac{60f}{p_{PM} + q} \tag{10}$$

Among them, f is the frequency through the AC armature winding. The synchronization speed of the PPMLM can be expressed as follows

$$v_s = \frac{D}{2} \cdot \frac{2\pi n_r}{60} = \frac{D}{2} \cdot \frac{2\pi}{60} \cdot \frac{60f}{p_{PM} + q} = \frac{\pi Df}{p_{PM} + q} = \frac{L_a f}{N_r} \tag{11}$$

Where, D is the diameter of the stator circle in the rotating motor, Nr is the synchronous number in the rotating motor. When the PPMLM is used as an electromotor, the armature winding is connected in a series with frequency converter, and then controlling the frequency of the armature winding can influence the speed of the motor.

C. The type of the winding(concentrated with)

In this paper, 12 permanent magnets and 8 armature windings placed on the primary structure, and the number of grooves per phase per pole is 0.5. To reduce the length of the winding end, the concentrated winding can be used, which is expressed as Fig. 3.

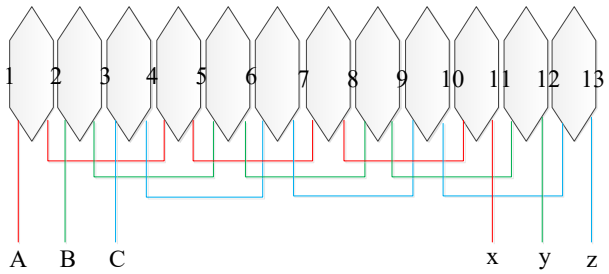

Fig. 3. The type of the winding(concentrated with)

The key parameters of the motor can be shown in the following table 1：

Table 1

Key parameters of the PPMLM

Machine Parameter	Value
Number of PM poles	12
Number of primary teeth	12
Number of Primary grooves	12
Phase number	3
Primary side length/mm	1500
Air-gap length/mm	1

Through theoretical analysis, the operation principle of the motor is verified, which is also the prerequisite for further magnetic field analysis.

4. The analysis of magnetic coupling ability

Based the mathematical model presented in chapter 3, it can be seen that there is no direct coupling relationship between the armature windings and permanent magnets of PPMLM. Electromechanical energy is achieved by secondary coupling of their magnetic fields, and secondary acts as the pole to digital converter. The secondary coupling ability has a great influence on the motor's performance, so determining the secondary structure parameters of the motor is very important. In this part, the effect of the pole pitch factor on PPMLM coupling ability is analyzed.

A. The influence of the salient pole's arc-coefficient on flux linkage

Arc-coefficient of the salient pole is one of the major parameters of the secondary structure. The pole pitch factor determines its size of air gap between the convex poles, thus affecting the secondary coupling capability. A parametric model of motor with pole arc-coefficient 0.3-0.9 increment of 0.1 is established under the same motor structure size and operating conditions for analyze the function of motors with different pole pitch factors. When the permanent magnet is excited

separately, the finite element analysis of different pole pitch factors is carried out. The fundamental wave is a magnetic component, the pole pairs number of fundamental waves equals the number of the permanent magnet. The useful harmonic is a magnetic component with the same number of pole pairs as the armature winding. The Fourier decomposition of the air gap magnetic flux density is used to analyze the changes of 8 magnetic field components and 12 poles magnetic field components, as shown in Fig. 4.

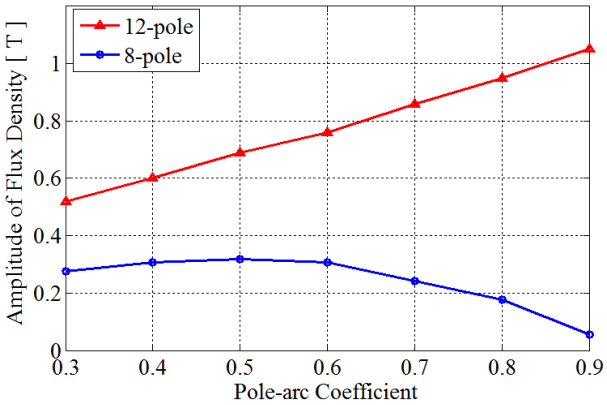

Fig. 4. Amplitude of flux density with the different pole arc coefficient

The coupling ability of the motor is studied by analyzing the magnetic component. Take the air gap magnetic flux density in the middle of the air gap. Fig. 4 shows that, as the pole arc coefficient increases, the magnitude of 12 magnetic field component increases continuously, and the 8th harmonic magnetic field component increases first, after 0.6, it starts to decrease. In order to obtain a larger back electromotive force, the pole arc-coefficient of 8 times larger harmonic magnetic field component should be selected. At the same time, the influence of the variation of the number of magnetic layers on the modulation capacity of the motor is also considered. Therefore, the initial selection of the pole arc coefficient is 0.4-0.6. Meanwhile, considering the impact of the variation of the layer number on coupling ability, the initial selection range of the pole arc coefficient is 0.4-0.6.

B. The influence of the number of permeance layers on the effective harmonic content

The magnetic barrier secondary consists of a magnetic reluctance layer and a non performance layer. The number of magnetic reluctance layers has a great effect on the modulation of the magnetic field, and the rational selection of magnetic space is also an important factor to strengthen the modulation capacity of the magnetic field.

The PPMLM finite element model of 1-6 layers of magnetic space is established, and the finite-element method(FEM) is analyzed. The air gap flux

density is decomposed by the Fourier technique when the permanent magnet is excited separately, as shown in Fig. 5, and the figure of 8 extremely effective harmonics can be obtained.

Fig. 5 shows that, with the increase of the magnetic reluctance layer and the number of barrier layers, the percentage of useful harmonics is increasing. As the number of the magnetic space layers increases, the number of non-permeance layer also increases, and the ability of magnetic modulation is increasing, so the secondary magnetic field modulation effect is better. However, an excessive number of nonmagnetic layers will increase secondary magnetic circuit saturation, reduce secondary modulation ability, and also increase the difficulty and cost of processing. When the number of plies is 3 layers above, the modulation capacity of the magnetic field varies little. Because of the manufacturing cost and the saturation of the secondary magnetic circuit, the secondary permeance layer is selected as a 3~4 layer.

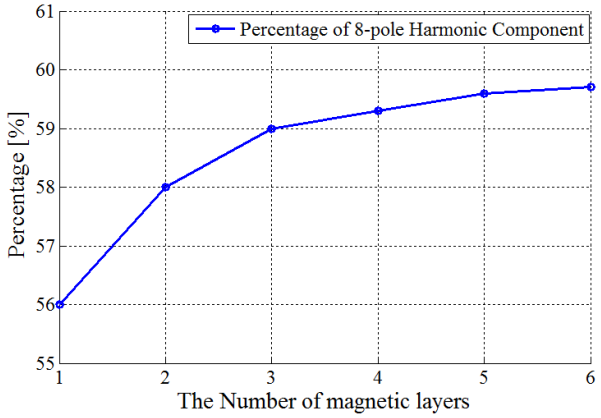

Fig. 5. Percentage of 8-pole harmonic component

C. Influence of permanent magnet thickness on no-load induced EMF

Permanent magnets are available in sizes ranging from 0.5 to 5.5 mm, with a step size of 0.5 mm. PPMLM carries out the no-load simulation, and the simulation results are analyzed. The increase in permanent magnet thickness has no linear relationship with the change of the back EMF amplitude of PPMLM, as seen in Fig. 6. The slope of the curve is larger when the permanent magnet thickness is 0.5 ~ 2mm, and the contribution of the thickness of the permanent magnet to the induced EMF of the motor is larger. The slope of the curve reduces as the permanent magnet thickness is 2 ~ 4mm, and the change in back EMF of the motor slows down. After 4mm, the thickness of the permanent magnet decreases. The contribution increase of thrust amplitude to the increase of thrust amplitude is relatively small. In consideration of the magnetic circuit saturation, the thickness of the permanent magnet should not be too large, to prevent magnetic circuit saturation. At the same time, if the thickness of the permanent magnet is too thin, it

is prone to irreversible demagnetization, so the thickness of the permanent magnet should be moderate. In this thesis, the permanent magnet thickness in this thesis is 4mm, and PPMLM has good performance.

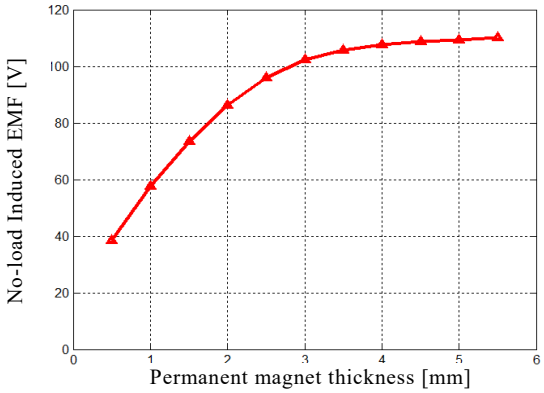

Fig. 6. Influence of permanent magnet thickness on no-load induced EMF

D. Influence of opening width of primary groove on positioning force

The no-load simulation of the motor is carried out. Fig. 7 is the curve of the peak value of the position force changing with the groove opening width. The peak value of the position force varies with the groove opening width, as seen in the figure. When the groove opening width is 10 mm, the peak value of the positioning force reaches the minimum. Therefore, the groove opening width of 10 mm is taken as the primary groove opening width of PPMLM, and the motor performance is better in this time. Which makes the motor performance better.

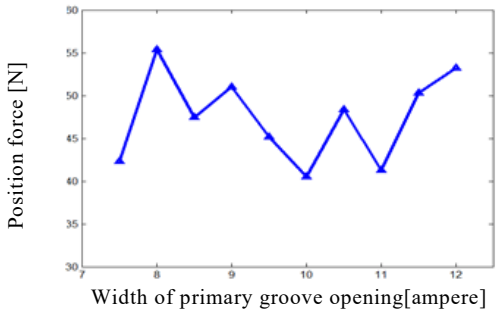

Fig. 7. Influence of primary notch width on positioning force }

5. Static characteristic

A. magnetic flux density diagrams

When the permanent magnet is separately excited and the armature winding is open, the no-load running state of the motor is evaluated using finite element

method, and then the correlation analysis results are obtained. Fig. 8 shows the distribution of the streamlines of the PPMLM is presented.

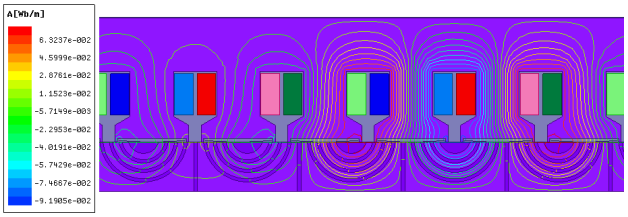

Fig. 8. The Magnetic force line distribution

From Fig. 9, the magnetic flux density distribution of the PPMLM can be shown. Through analysis, we can see that the magnetic distribution of primary teeth, the yoke and secondary parts are rational, so as to meet the design requirements.

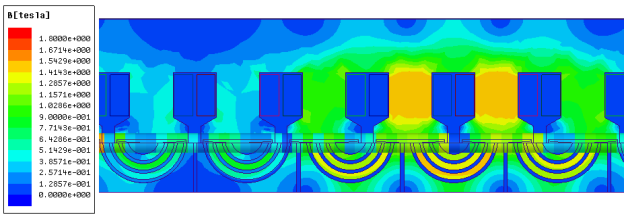

Fig. 9. No-load magnetic flux density distribution

B. The No-load back EMF

The no-load back of EMF is an important sign of the motor's performance. When no-load, the magnitude of the back EMF reflects the rationality of the pole number of the winding and the load-carrying capacity of the motor. Fig. 10 shows the no-load flux linkage of the three-phase winding. In Fig. 11, the no-load EMF waveform of the three-phase winding, and the harmonic content of the EMF is less. As you can see from the diagram, the degree of sine is relatively high.

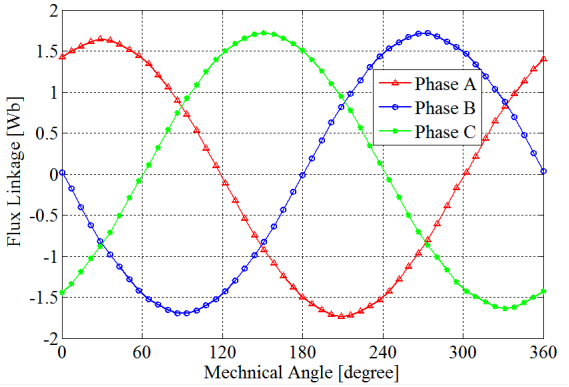

Fig. 10. No-load flux Linkage

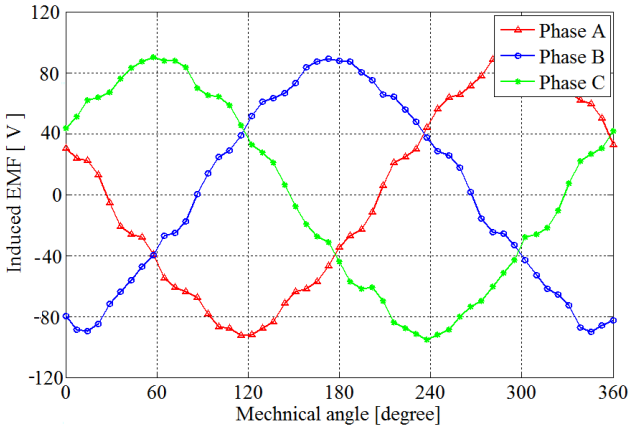

Fig. 11. No-load induced EMF

C. The flux density decomposition of the air gap

Based on the finite element method, the gap density and the magnetic field of PPMLM are analyzed, meanwhile, the air-gap flux density in vertical direction is obtained. Fig. 12 shows that, Fourier transform is used to decompose 8 effective harmonic magnetic flux density sinusoidal waveforms. For motor operation, the 8 useful harmonics is used as an effective air gap magnetic field, the larger induced electromotive force and thrust density also can be obtained.

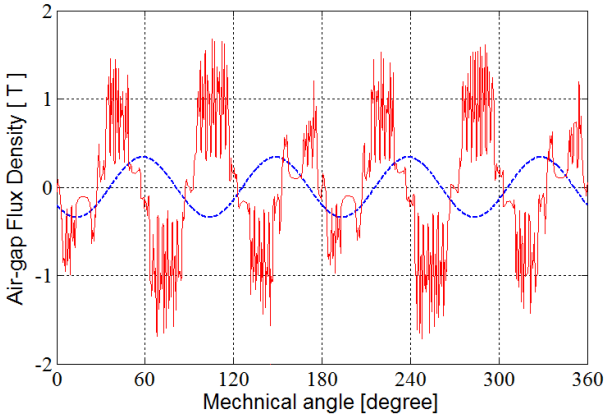

Fig. 12. No-load air gap flux density

Fig. 13 shows the harmonic analysis of the air gap magnetic field. To explain the problem more accurately, the air gap magnetic field harmonic analysis method is adopted. The abscissa is the polar logarithm of the harmonic magnetic field.

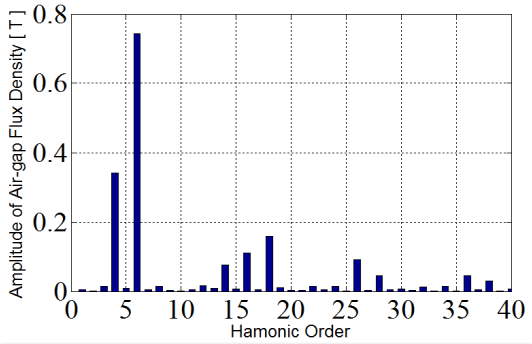

Fig. 13. Air-gap magnetic flux FFT

Fig. 13 shows that the 6th harmonic and 4th harmonic are large, thus, other harmonics are lower according to FFT spectrum. From the results of simulation, the magnetic flux field of the permanent magnet is more reasonable after secondary modulation.

D. Analysis of electromagnetic thrust

The current will affect the motor thrust. Fig. 14 shows the average thrust versus peak current. It can be seen that the point of 6 amperes is the turning point of this curve. When the peak current is less than 6 amperes, due to the linear characteristics of ferromagnetic materials, as the input current increase, the thrust of the motor increases greatly, showing a linear change. However, when the peak current is more than 6 amperes, the increase of thrust gradually tends to be flat due to the increase in magnetic circuit saturation. When the PPMLM is rated at 6 amperes, the motor has a wide linear overload zone.

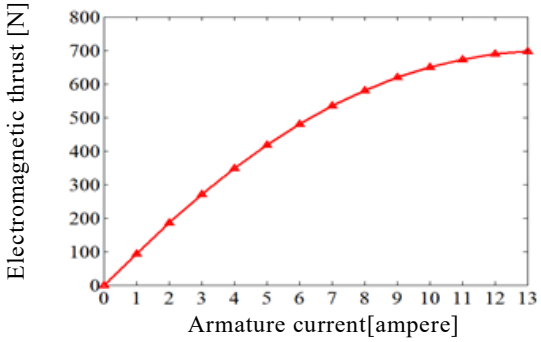

Fig. 14. The effect of the armature current on the thrust

6. Experimental model

As shown in Fig.15, the experimental platform is composed of linear motor, PC computer, Driver and WNMC400 motion controller. PPMLM prototype

parameters are provided in Table 1. WNMC400 motion controller is a real-time control system, which can interact with PC directly through serial port line. The maximum pulse output frequency can reach 2MHz. Its control core is composed of a new generation of corexm3 high-performance processor and FPGA. The current signal is measured by Hall switch sensor, and the speed and position signals are measured by incremental grating ruler. After the prototype platform of linear motor is built, the thrust test experiment is carried out. The comparison between the measured and calculated thrust values is shown in Figure 16. The calculated and measured values of the motor are in good agreement, and the operation is relatively stable.

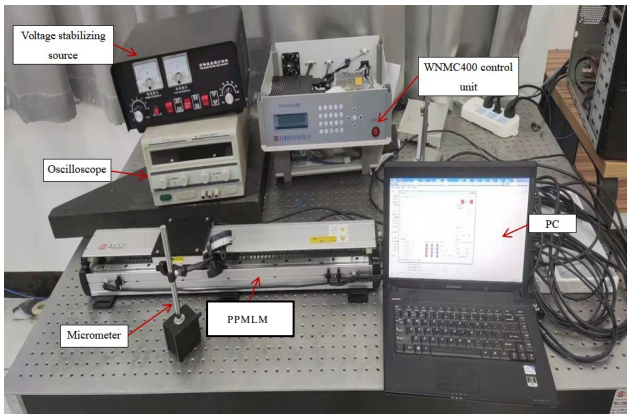

Fig.15 PPMLM experimental platform

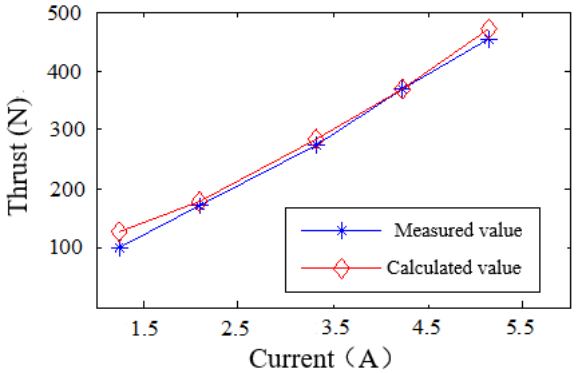

Fig.16 PPMLM experimental platform

7. Conclusions

PPMLM is a new type of motor, and PPMLM is proposed and designed in this article, and the principle of PPMLM is introduced in detail, and the air-gap flux density equation and synchronous speed equation of the motor are calculated. By analyzing the influence of the pole pitch factor and the number of guiding magnetic layers on the harmonic content, it can be concluded that the initial selection range of the pole pitch factor is 0.4-0.6, meanwhile, the motor structure with 3-4 guiding magnetic layers is relatively better. When studying the static characteristics of PPMLM, the flux linkage, counter EMF and electromagnetic thrust of the motor are analyzed. The results show that higher effective harmonics can be obtained based on the significant modulation effect, and the effective harmonics can generate larger no-load counter EMF and electromagnetic thrust. Some deficiencies also exist in the new motor, for example, thrust fluctuation needs to be further suppressed, and the appropriate dedicated control system is not perfect. Through the above analysis, this motor is especially suitable for long-distance rail transit system, has a very broad development prospect, and provides valuable reference value for linear drive research. The prototype platform of PPMLM is built and verify the effectiveness of theoretical analysis.

Acknowledgments

The project is funded by the National Natural Science Foundation of China (51777127), Scientific research projects in Liaoning Province (2020-MS-240), Shenyang talent project (RC200192), Liaoning Provincial Department of education project (LJKZ1085).

REFERENCES

[1]. *W. Ji*, *G. Jeong*, *C. Park*, *I. Jo* and *H. Lee*. “A study of non-symmetric double-sided linear induction motor for hyperloop all-in-one system (propulsion, levitation, and guidance)”. IEEE Trans. Magn., vol. 54, no. 11, pp. 8207304, 2018.

[2]. *X. T. Li*, *G. T. Ma* et al. “Numerical modeling and transient analysis of a linear induction motor with close-ended coated superconductor coils as secondary”. IEEE Trans. Appl. Supercond., vol. 27, no. 3, pp. 5203307, 2017.

[3]. *Han Yongchun*. “Study on the relationship between air gap and train energy consumption of linear motor”. Railway Rolling Stock, vol. 35, no. 6, pp.69-72, 2015.

[4]. *Jo J M*, *Lee J H*, *Han Y J*, et al. “Development of Propulsion Inverter Control System for High-Speed Maglev based on Long Stator Linear Synchronous Motor”. Energies, MDPI, vol. 10, no. 6, pp.1-9, Feb. 2017.

[5]. *R. Cao*, *M.Lu*, *N. Jiang* and *M. Cheng*, "Comparison between linear induction motor and linear flux-switching permanent-magnet motor for railway transportation," IEEE Trans. Ind. Electron., vol. 66, no. 12, pp. 9394-9405, Dec. 2019.

[6]. *Lu Q*, *Yao Y*, *Shi J*, et al. “Design and performance investigation of novel linear switched flux PM machines”. IEEE Trans. Ind. Appl., vol. 53, no. 5, pp. 4590-4602, 2017.

[7]. *Tanaka, C.N.*, *Chabu*. "Flux Reversal Free Splittable Stator Core Doubly Salient Permanent Magnet Motor," IEEE Latin America Transactions, vol. 18, no. 8, pp. 1329-1336, Aug. 2020.
[8]. *Lounthavong*, *V., Sriwannarat*, *W., Siritaratiwat*, *A., Khunkitti*. "Optimal Stator Design of Doubly Salient Permanent Magnet Generator for Enhancing the Electromagnetic Performance," Energies, vol. 12, no. 6, pp. 3201-3213, Aug. 2019.
[9]. *ABDUL WAHEED* and *JONG-SUK RO*. "Analytical Modeling for Optimal Rotor Shape to Design Highly Efficient Line-Start Permanent Magnet Synchronous Motor". IEEE access, vol. 8, pp. 145672-145686, Aug. 2020.
[10]. *X. Zhu*, *J. Ji*, *L. Xu* and *M. Kang*. "Design and analysis of dual-stator PM vernier linear machine with PMs surface-mounted on the mover". IEEE Trans. Appl. Supercond., vol. 28, no. 3, pp. 5201605, 2018.
[11]. *A. Nematsaberi* and *J. Faiz*. "A novel linear stator-PM vernier machine with spoke-type magnets". IEEE Trans. Magn., vol. 54, no. 11, pp. 8106905, 2018.
[12]. *N. Baloch*, *B. Kwon* and *Y. Gao*. "Low-cost high-torque-density dual-stator consequent-pole permanent magnet vernier machine". IEEE Trans. Magn., vol. 54, no. 11, pp. 8206105, 2018.
[13]. *O. Farrok*, *M. R. Islam*, *Y. Guo*, *J. Zhu*, *W. Xu*. "A novel design procedure for designing linear generators". IEEE Trans. Ind. Electron., vol. 65, no. 2, pp. 1846-1854, 2018.
[14]. *W. Wang*, *Y. Feng*, *Y. Shi*, *M. Cheng*, *W. Hua* and *Z. Wang*, "Direct thrust force control of primary permanent-magnet linear motors with single DC link current sensor for subway applications," IEEE Trans. Power Electron., vol. 35, no. 2, pp. 1365-1376, Feb. 2020.
[15]. *M. Khayamy* and *H. Chaoui*, "Current sensorless MTPA operation of interior PMSM Drives for vehicular applications," IEEE Trans. Veh. Technol., vol. 67, no. 8, pp. 6872-6881, Aug. 2018.
[16]. *W. Wang*, *Y. Feng*, *Y. Shi*, *M. Cheng*, *W. Hua* and *Z. Wang*, "Fault-tolerant control of primary permanent-magnet linear motors with single phase current sensor for subway applications," IEEE Trans. Power Electron., vol. 34, no. 11, pp. 10546-10556, Nov. 2019.